RSC Sustainability

ROYAL SOCIETY OF CHEMISTRY

PAPER

View Article Online
View Journal | View Issue

Cite this: *RSC Sustainability*, 2026, **4**, 1867

A group contribution approach for predicting the environmental impacts of imidazolium-based ionic liquids

Mirco Volanti,[a] Piya Gosalvitr,[b] Carlos Avendaño,[b] Adam J. Greer,[b] Christopher Hardacre,[b] Fabrizio Passarini[ac] and Rosa M. Cuéllar-Franca[*b]

In this work, the environmental impacts of imidazolium-based ionic liquids (ILs) are estimated and predicted by combining life cycle assessment (LCA) and a linear group contribution (GC) model to make this information readily available and accessible at early stages of ILs design and selection. This study has resulted in the development of predictive models for global warming, human toxicity and eco-toxicity impacts of imidazolium-based ILs with high accuracy. The validated models are based on the environmental impact data of a sample of 30 ILs with the same cation head group, which was estimated as part of this study using the LCA methodology. The sample considered variations in the cation's hydrocarbon chains, *e.g.* alkyl, aromatic, multiple side chain and chain length variations, and the commonly used anions chloride (Cl^-), tetrafluoroborate ($[BF_4]^-$) and hexafluorophosphate ($[PF_6]^-$), and it was assumed that the ILs were synthesised *via* alkylation and salt metathesis reactions. Both LCA and GC models results show a clear distinction between the environmental impacts of imidazolium chloride, imidazolium tetrafluoroborate, and imidazolium hexafluorophosphate ILs in the order $Cl^- < BF_4^- < PF_6^-$, thus indicating the large influence of the anion when it comes to their environmental sustainability performance. For example, the global warming potential of the ILs per kg are 2 and 3 times higher when substituting the chloride anion with $[BF_4]^-$ and $[PF_6]^-$ anions, respectively. It is recommended that the sample be expanded to include ILs from other head groups, compare alternative synthesis routes and include purification steps to extend the analysis.

Received 8th August 2025
Accepted 19th February 2026

DOI: 10.1039/d5su00658a

rsc.li/rscsus

Sustainability spotlight

Ionic liquids are versatile organic salts that offer safer, cleaner, and more efficient alternatives to conventional solvents. However, assessing their life cycle environmental sustainability is under-researched, as data scarcity and system complexity make LCAs time-intensive. This work, for the first time, applies predictive tools to estimate environmental sustainability properties, presenting a proof of concept that correlates impacts (*e.g.*, global warming potential) with functional chemical groups added at each synthesis step. This work will enable the specialised chemicals community to screen candidates for both functional properties and environmental performance at early design stages. Embedding such quantitative metrics into accessible predictive frameworks advances sustainable innovation, supporting SDGs 9, 12, and 13[1], allowing industry to integrate sustainability at the heart of innovation strategies.

1 Introduction

Ionic liquids (ILs) are organic salts with low melting points, typically below 100 °C, that offer industry endless possibilities for sustainable innovation thanks to their unique and tuneable physicochemical properties including low vapour pressures, high thermal stability, good electrical conductivity, and wide electrochemical window.[1,2] For example, ILs are being examined to replace conventional solvents, catalysts and electrolytes, as well as additives in formulated products such as lubricants, paints, *etc.* to develop safer, cleaner and more efficient technologies across various applications that can contribute towards reaching Net Zero.[2] These applications include biomass transformation, *e.g.* catalytic conversion of biomass into fuels and value-added chemicals,[3] gas capture and storage, *e.g.* carbon capture and other acidic gases,[4–7] and energy storage and conversion devices.[8] ILs have also been commercialised in the process industries as reported in various comprehensive reviews,[2,9,10] where a more extensive list of applications and detailed descriptions can be found. For instance, notable commercial or pilot industrial applications include the BASF BASIL™ technology for acid scavenging, the Chevron/

[a]*Department of Industrial Chemistry "Toso Montanari", Bologna University, Via Piero Gobetti 85, 40129 Bologna, Italy*

[b]*Department of Chemical Engineering, The University of Manchester, Oxford Rd., Manchester M13 9PL, UK. E-mail: rosa.cuellarfranca@manchester.ac.uk*

[c]*Centro Interdipartimentale di Ricerca Industriale – Fonti Rinnovabili, Ambiente, Mare ed Energia, Via Angherà 22, 47900 Rimini, Italy*

Honeywell UOP ISOALKY™ alkylation technology for cleaner motor fuels, the PETRONAS HycaPure® process for mercury removal from natural gas, the Mari Signum IL-based technology for chitin extraction from shellfish, and the ionoSolv biomass fractionation technology.[11–13]

With around 500 ILs currently produced commercially at various scales,[2] and with a vast number of possible cation and anion combinations,[1,9] extensive computational modelling work has been carried out on the prediction of physical properties (*e.g.* melting point, density, viscosity), solubility of gases and toxicity of ILs.[14] Examples of predictive-correlative methods include quantitative structure–property relationship (QSPR), quantitative structural–activity relationship (QSAR), molecular simulation methods,[15,16] molecular-based equations of state,[17] and group contribution (GC) models, which rely on experimental and/or theoretical measurements or different types of molecular descriptors (*e.g.* molecular structure, activity coefficients, dipole moment, atomic charges, polarizability, σ-profiles, *etc.*) as training data.[14] Both QSPR and QSAR are mathematical models used for establishing relationships between chemical descriptors of substances and properties or biological activities, respectively.[14,18] In both molecular simulations and molecular-based equations of state, the properties of the molecules are determined from knowledge of the intermolecular forces using statistical mechanics methods.[15] GC models, on the other hand, are semi-empirical approaches that break down molecules into functional chemical groups, each of them contributing to the property of interest in a certain mathematical functional form that depends on the specific property being represented.[19,20] QSPR, molecular simulations, molecular-based equations of state, and GC models have been mostly used in predicting the physicochemical properties of ILs,[14,21] whilst QSAR models have been employed to predict the toxicity of ILs.[18] The ability to predict such properties has enabled the IL research community to screen and design suitable ILs candidates for specific applications. However, current property prediction, and consequently, screening methods are task-oriented and do not consider upstream burdens, such as the environmental impacts associated with their production.[22] Moreover, ILs toxicity predictive models are limited to describing the intrinsic properties of ILs on damaging organisms, leaving out the effects of the different precursors involved in the synthesis of ILs and any other stages in their life cycle.

The negligible volatility of ILs has largely contributed to the perception that ILs are "green solvents", however, other sustainability metrics assessing key aspects such as their synthesis, recyclability and disposal should also be considered to enable sustainable chemical processes innovations and fully unlock their "transformative" potential.[13] ILs synthesis typically requires several steps involving numerous precursors that may result in higher environmental impacts compared to conventional solvents as evidenced by several emerging LCA studies in this field.[22–30] Nevertheless, the quantification of the environmental impacts of hundreds of ILs, given the vast number of possible ILs combinations, can become a taxing task that requires specialised knowledge and significant resources, including data on the synthesis of complex chemical precursors if unavailable in commercial LCA databases, making traditional LCA approaches impractical to implement at early stages of IL design. ILs manufacturing data availability at a commercial scale remains largely unknown due to a lack of process data, thus limiting available LCA studies of ILs, which mostly rely on laboratory-scale data combined with stoichiometric and other engineering calculations,[22–25,27,30] and process simulation tools,[26,28,29] to obtain life cycle inventories at various scales. These studies reported the environmental impacts of the production of one or two ILs alongside a competing conventional solvent (in most instances) to provide comparative assessments per unit of mass. Collectively, these studies offer a limited coverage of cation head groups, *e.g.* imidazolium-, ammonium- and phosphonium-based ILs, and anions, *e.g.* carboxylates, halides, inorganic fluorinated and acid anions, with the cation 1-butyl-3-methylimidazolium being the most widely assessed to date. For example, the estimated global warming potential (GWP) of 1-butyl-3-methylimidazolium ILs ranges between 3.5 and 7.4 kg CO_2 eq. per kg IL depending on the anion and synthesis pathway,[22] which is much higher compared to the GWP of conventional solvents such as hexane and methanol (from syngas), which are reported at 0.54 kg CO_2 eq. per kg hexane and 0.61 kg CO_2 eq. per kg methanol, respectively.[31] A more detailed discussion of existing LCA studies has been presented previously,[22] and also discussed in Section 3.1.4. More recent literature has expanded the scope of LCA studies by comparing ILs synthesis pathways and by integrating application-stages impacts,[29] as well as by quantifying uncertainty in both background and foreground life-cycle inventories to improve reliability of identified hotspots and interpretation of environmental impact results for ILs.[28]

Recent studies have demonstrated the application of GC methods for the prediction of environmental impacts, *e.g.* global warming and ozone depletion, and other environmental and safety-related properties, *e.g.* atmospheric lifetime and minimum ignition energy, of conventional chemicals using molecular structure data to develop several regression methods for their analysis and measurement in the absence of experimental data.[32,33] Even though these methods relied on limited data sets, the accuracy of the resulting models was good, thus enabling fast access to environmental-related and safety metrics needed to design more environmentally sustainable and safer processes. Similar to the work reported for conventional chemicals, GC methods can be used to construct mathematical models to predict the environmental impacts of ILs production using correlations between their chemical structure and the environmental impacts of the various steps in their synthesis. The present study aims to demonstrate the application of GC methods in the prediction of environmental impacts of ILs synthesis, therefore expanding the existing predictive-correlative methods toolkit for ILs property prediction to include environmental sustainability metrics such as global warming, making these data readily available and accessible to scientists and engineers at early stages of IL design. Whilst the environmental impacts of single ILs estimated in standalone LCA studies previously discussed serve as a starting point for understanding the

environmental sustainability challenges in ILs production, this information alone is insufficient to establish patterns, and traditional approaches become impractical when screening hundreds of IL combinations. This study proposes the use of imidazolium-based ILs to establish a proof of concept for the prediction of environmental impacts, by selecting a representative sample of 30 different imidazolium-based ILs that includes different cationic side chain substituents and types of connections, *e.g.* branching, double bonds, and three different anions. Imidazolium-based ILs were selected as the head group because these are the most widely studied and applied family of ILs.[34] This ensured sufficient data availability for estimating the environmental impacts of the sample using the LCA methodology, and the extensive availability of physical properties and toxicity data, combined with their widespread use in the research community, makes the resulting predictive models relevant and readily applicable. As far as the authors are aware, this represents the first attempt to predict environmental impacts of ILs using GC or any other methods. Having access to environmental impact data on ILs production in a practical and timely manner, alongside physical properties and toxicity information, will enable researchers and ILs manufacturers to screen and design more environmentally sustainable ILs, a much-needed step towards their commercial application in a Net Zero technological landscape.

2 Methodology

The methodology used in this study comprises the following four main steps: (i) selection of the IL sample; (ii) selection of synthesis route and identification of main synthesis steps; (iii) environmental impact assessment of the IL sample; and (iv) group-contribution analysis and validation. These steps are described over the next sections.

2.1 Ionic liquid sample selection

The first step in the methodology is the selection of a representative sample of ILs from the same family. In this study, the imidazolium head group was selected to demonstrate the methodology as this is the most widely studied family of ILs[34] and is more likely to find the necessary inventory data for the environmental impact assessment step described in Section 2.3. A sample of 30 different imidazolium-based ILs was selected as shown in Table 1. The sample considered variations in the cation's hydrocarbon chains based on literature[35] *e.g.* alkyl, aromatic, multiple side chain and chain length variations, and commonly used anions, *i.e.* chloride (Cl^-), tetrafluoroborate ($[BF_4]^-$) and hexafluorophosphate ($[PF_6]^-$) anions. The selected sample is designed to ensure, as far as possible, that chemical groups are repeated across different molecules, thereby promoting the transferability of GC model parameters throughout the entire sample; that is, the contribution of a given chemical group to a specific environmental impact is assumed to be independent of the molecule in which it appears.

2.2 Selection of synthesis route and identification of main synthesis steps

The next step in the methodology is the selection of the most prevalent commercial processes for synthesising the ILs under study, and the identification of their corresponding main synthesis steps to generate the necessary data for the LCA and GC analysis. Imidazolium-based ILs can be synthesised *via* combination of alkylation, acid–base neutralisation, anion/salt metathesis, and ion-exchange.[34] Halide-free route alternatives have also been suggested in the literature.[22,29] This study considered the preparation of the imidazolium-chloride ILs *via* an alkylation reaction, followed by a salt metathesis to prepare the imidazolium-tetrafluoroborate and imidazolium-hexafluorophosphate ILs, to demonstrate the proof-of-concept. These methods were selected because they are the most used methods for the synthesis of ILs.[34] For the purpose of this proof of concept, the selected synthesis route was divided into four distinctive steps, starting from the formation of the imidazolium ring, followed by the methylation, alkylation and metathesis as shown in Fig. 1 and 2. This level of disaggregation was required from an LCA perspective due to the limited availability of ILs precursor data in commercial databases such as Ecoinvent. As a result, the imidazolium ring formation and methylation steps were explicitly included prior to the alkylation and metathesis reactions, enabling the application of a group-contribution approach for the prediction of the environmental impacts of ILs. These steps are described in detail in the next sections.

2.2.1 Imidazole ring formation. This step represents the starting point for all imidazolium-based ILs studied here, where glyoxal reacts with formaldehyde (or acetaldehyde in the case of 1-butyl-2,3-dimethyilimidazolium to obtain the methyl group on the second position of the ring), and ammonia to form the imidazole ring as shown in Fig. 2(a), *via* the Debus–Radziszewski synthesis method.[36] This reaction is typically conducted in the presence of water at temperatures between 50 °C and 100 °C, with an imidazole yield in the range of 60–85% and achieving a purity over 99% *via* distillation. In this study, the reaction is assumed to occur at 75 °C with a product yield of 85%.

2.2.2 Methylation. The imidazole ring undergoes methylation with methyl chloride to produce 1-methylimidazole, first alkylation step as described in Fig. 2(b). This step is common to all the ILs listed in Table 1, and in the case of [Hmim]Cl, this is the only step. The synthesis of selectively substituted imidazoles with alkyl halides has been reported in the literature under high temperatures (*e.g.* 100 °C) in the presence of water, with the highest reported yield being 76%.[37,38] These conditions were assumed for the purpose of this study.

2.2.3 Alkylation. Finally, the IL is formed in a second alkylation step, illustrated in Fig. 2(c), in which a second or third substituent, depending on the IL, is introduced to the imidazolium ring using an alkyl chloride to produce the chloride-based IL. The alkyl chloride is used in stoichiometric excess to ensure complete formation of the alkylated imidazolium cation and to facilitate removal of unreacted starting

Table 1 Selected sample of ILs from the imidazolium head group

Ionic liquid	R_1[a]	R_2[a]	R_3[a]	X^-[b]	Abbreviation
1-Methylimidazolium chloride	Methyl	—	—	Cl^-	[Hmim]Cl
1-Methylimidazolium tetrafluoroborate	Methyl	—	—	$[BF_4]^-$	[Hmim][BF_4]
1-Methylimidazolium hexafluorophosphate	Methyl	—	—	$[PF_6]^-$	[Hmim][PF_6]
1-Ethyl-3-methylimidazolium chloride	Ethyl	—	Methyl	Cl^-	[C_2mim]Cl
1-Ethyl-3-methylimidazolium tetrafluoroborate	Ethyl	—	Methyl	$[BF_4]^-$	[C_2mim][BF_4]
1-Ethyl-3-methylimidazolium hexafluorophosphate	Ethyl	—	Methyl	$[PF_6]^-$	[C_2mim][PF_6]
1-Butyl-3-methylimidazolium chloride	Butyl	—	Methyl	Cl^-	[C_4mim]Cl
1-Butyl-3-methylimidazolium tetrafluoroborate	Butyl	—	Methyl	$[BF_4]^-$	[C_4mim][BF_4]
1-Butyl-3-methylimidazolium hexafluorophosphate	Butyl	—	Methyl	$[PF_6]^-$	[C_4mim][PF_6]
1-Hexyl-3-methylimidazolium chloride	Hexyl	—	Methyl	Cl^-	[C_6mim]Cl
1-Hexyl-3-methylimidazolium tetrafluoroborate	Hexyl	—	Methyl	$[BF_4]^-$	[C_6mim][BF_4]
1-Hexyl-3-methylimidazolium hexafluorophosphate	Hexyl	—	Methyl	$[PF_6]^-$	[C_6mim][PF_6]
1-Octyl-3-methylimidazolium chloride	Octyl	—	Methyl	Cl^-	[C_8mim]Cl
1-Octyl-3-methylimidazolium tetrafluoroborate	Octyl	—	Methyl	$[BF_4]^-$	[C_8mim][BF_4]
1-Octyl-3-methylimidazolium hexafluorophosphate	Octyl	—	Methyl	$[PF_6]^-$	[C_8mim][PF_6]
1-Decyl-3-methylimidazolium chloride	Decyl	—	Methyl	Cl^-	[C_{10}mim]Cl
1-Decyl-3-methylimidazolium tetrafluoroborate	Decyl	—	Methyl	$[BF_4]^-$	[C_{10}mim][BF_4]
1-Decyl-3-methylimidazolium hexafluorophosphate	Decyl	—	Methyl	$[PF_6]^-$	[C_{10}mim][PF_6]
1-Allyl-3-methylimidazolium chloride	Allyl	—	Methyl	Cl^-	[Amim]Cl
1-Allyl-3-methylimidazolium tetrafluoroborate	Allyl	—	Methyl	$[BF_4]^-$	[Amim][BF_4]
1-Allyl-3-methylimidazolium hexafluorophosphate	Allyl	—	Methyl	$[PF_6]^-$	[Amim][PF_6]
1-Benzyl-3-methylimidazolium chloride	Benzyl	—	Methyl	Cl^-	[Bzmim]Cl
1-Benzyl-3-methylimidazolium tetrafluoroborate	Benzyl	—	Methyl	$[BF_4]^-$	[Bzmim][BF_4]
1-Benzyl-3-methylimidazolium hexafluorophosphate	Benzyl	—	Methyl	$[PF_6]^-$	[Bzmim][PF_6]
1-Phenyl-3-methylimidazolium chloride	Phenyl	—	Methyl	Cl^-	[Phmim]Cl
1-Phenyl-3-methylimidazolium tetrafluoroborate	Phenyl	—	Methyl	$[BF_4]^-$	[Phmim][BF_4]
1-Phenyl-3-methylimidazolium hexafluorophosphate	Phenyl	—	Methyl	$[PF_6]^-$	[Phmim][PF_6]
1-Butyl-2,3-dimethylimidazolium chloride	Butyl	Methyl	Methyl	Cl^-	[C_4dmim]Cl
1-Butyl-2,3-dimethylimidazolium tetrafluoroborate	Butyl	Methyl	Methyl	$[BF_4]^-$	[C_4dmim][BF_4]
1-Butyl-2,3-dimethylimidazolium hexafluorophosphate	Butyl	Methyl	Methyl	$[PF_6]^-$	[C_4dmim][PF_6]

[a] First, second and third alkylation positions, respectively as shown in Fig. 1. [b] Chloride (Cl^-), tetrafluoroborate ($[BF_4]^-$) and hexafluorophosphate ($[PF_6]^-$) anions.

materials. Different alkyl chlorides will result in the IL variations listed in Table 1. For example, the use of ethyl chloride and benzyl chloride will produce 1-ethyl-3-methyilimidazolium chloride and 1-benzyl-3-methyilimidazolium chloride, respectively. In this study, ethyl chloride, butyl chloride, hexyl chloride, octyl chloride, decyl chloride, allyl chloride, benzyl chloride and phenyl chloride were used to produce the ILs in the selected sample. Various synthesis protocols are reported in the literature, with the main differences related to reaction temperature and durations. For instance, Righi *et al.*[24] reported a reaction temperature of 80 °C for 36 hours, while Erdmenger *et al.*[39] used a microwave system at 170 °C for 11 minutes. Reported yields for these type of alkylation reactions range from

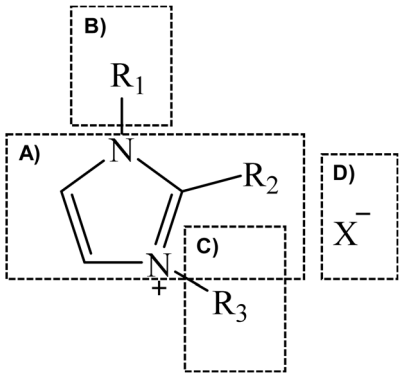

Fig. 1 Generic synthesis method in the production of alkyl-imidazolium ionic liquids, consisting of a ring formation (A), methylation (B), alkylation (C) and an anion metathesis (D) steps.

96.5 to 99%.[40] In this study, the higher reaction temperature and the upper end of the yield range were assumed.

2.2.4 Anion metathesis. The physiochemical properties of ILs can be tuned for specific applications by tailoring alkyl chain lengths on the cation, as well as the type of cation or anion.[34] In the case of varying the anion, the imidazolium chloride IL is subject to an anion metathesis to yield an IL with the desired anion.[41] In this study, $[BF_4]^-$ and $[PF_6]^-$ anions were considered to produce variations of the imidazolium-based ILs included in the selected sample. In this step, the imidazolium chloride IL reacts with either sodium tetrafluoroborate ($NaBF_4$)

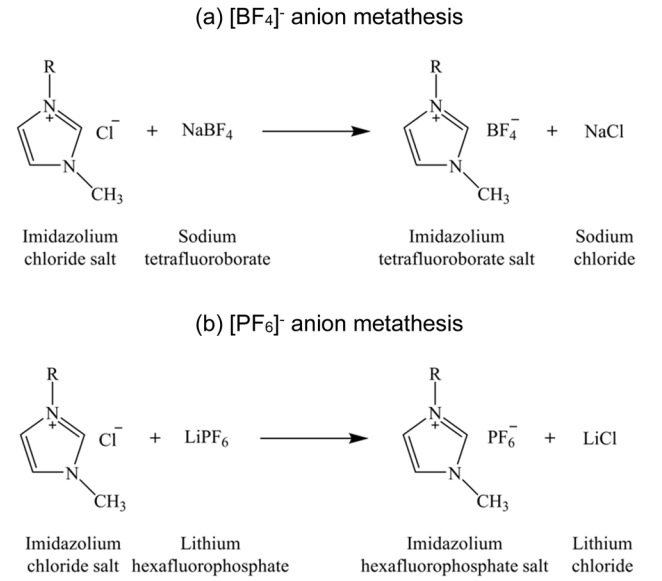

Fig. 3 Anion metathesis to produce (a) imidazolium tetrafluoroborate and (b) imidazolium hexafluorophosphate ILs.

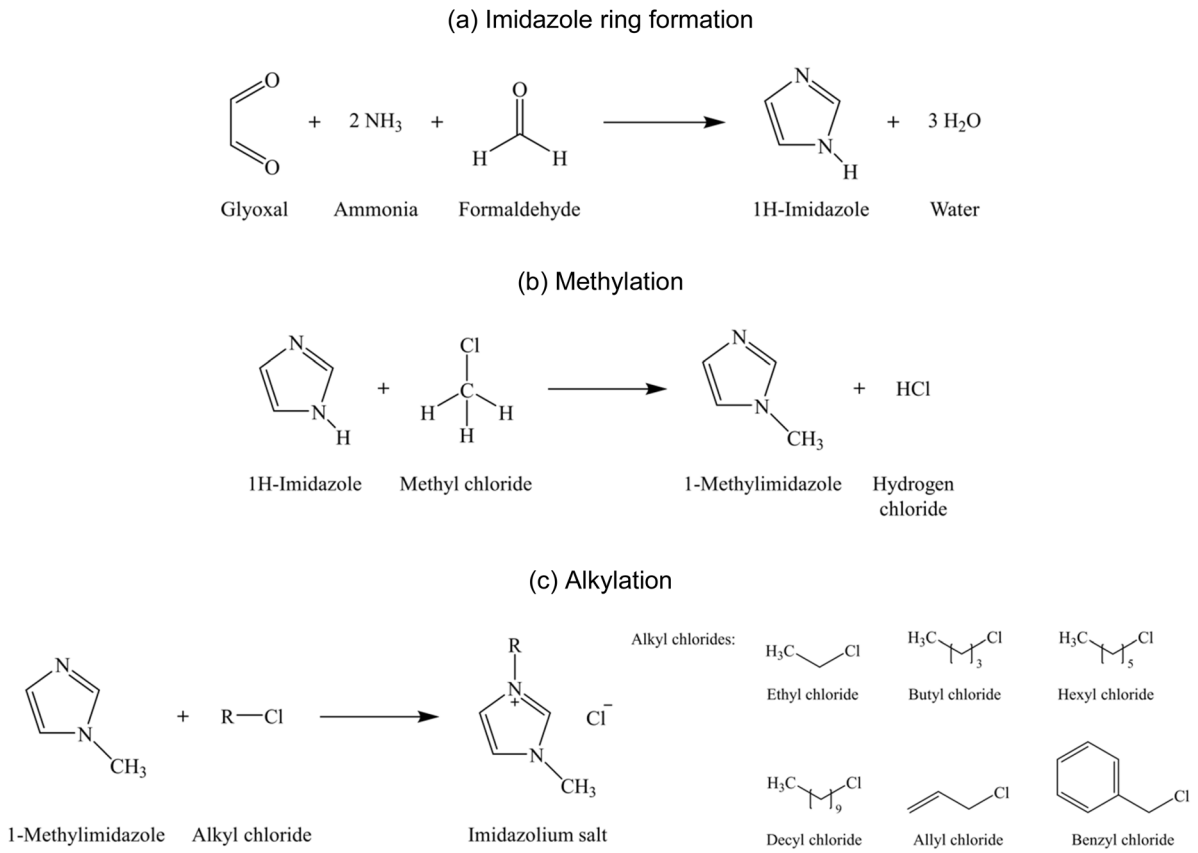

Fig. 2 Generic synthesis steps in the production of 1-alkyl-3-methylimidazolium chloride-based ILs. (a) Imidazole ring formation step; (b) methylation step; (c) second alkylation step and the various alkyl chlorides considered in the studied sample.

or lithium hexafluorophosphate ($LiPF_6$) to produce the desired ILs, as shown in Fig. 3. This step was included in order to provide a more representative pathway of the synthesis of ILs, which are commonly derived directly from an imidazolium halide precursor with the desired functionality.[42] The anion exchange reaction is typically carried out at room temperature, *i.e.* 25 °C, with yields of 91%,[41] which are the conditions assumed in this study.

The alkylation step corresponds to the final step in the synthesis of imidazolium chloride ILs, while the anion metathesis is an additional step needed in the synthesis of imidazolium tetrafluoroborate and imidazolium hexafluorophosphate ILs as discussed in this section. A purification and drying step would typically follow as a final stage in ILs synthesis.[34] However, this step was excluded from this study due to the wide range of purification methods reported in the literature, and the absence of disaggregated energy consumption data, which would introduce additional uncertainty. This limitation is further discussed in Section 3.3.

2.3 Environmental impact assessment of ILs

In this step, the environmental impact assessment data of ILs is estimated, which will be the basis of the GC models described in Section 2.4. Life cycle assessment (LCA) was used to calculate the environmental impacts of the 30 imidazolium-based ILs based on the ISO 14040 and 14044 guidelines,[43,44] as described next.

2.3.1 Goal and scope. The goal of this study was to estimate the environmental impacts of the 30 imidazolium-based ILs considered here, taking a closer look at the contributions and hotspots from their different synthesis steps. This is to establish correlations between functional chemical groups and environmental impacts of ILs. The system boundaries considered in this work are from "cradle-to-gate", as only the material and energy flows associated with the production of the ILs are of concern here, and the application, and disposal of ILs at their end-of-life falls outside the scope of this study. Contributions from purification and drying steps were excluded as previously explained. The impacts related to the chemical plant infrastructure and transportation of raw materials were excluded in this study as the contributions from these life cycle stages tend to be relatively small in chemical production compared to the continuous supply of raw materials and energy consumption.[45] The functional unit of "per mole of product" was selected to allow estimating the cumulative contributions of each synthesis step in the formation of the IL at a molecular level, and to prevent putting at disadvantage those ILs with lower molecular weights, *e.g.* more raw materials and energy resources would be required to produce one kg of IL resulting in a higher environmental burden. A second functional unit of "per kg of product" was also used to allow comparisons with other studies reported in the literature.

2.3.2 Life cycle inventory analysis. The inventory data used in the environmental assessment of the 30 ILs studied here are presented in Tables 2–5. In the absence of commercial scale data, the materials quantity data were obtained from stoichiometric calculations based on the synthesis steps and assumed conditions described in Section 2.2 (sample calculations are reported in the SI). A generic life cycle tree for the production of imidazolium-based ILs is given in Fig. 4, where the common precursors used in the synthesis of all ILs are identified. The energy consumption estimations followed the methodology proposed in Cuéllar-Franca *et al.*,[23] where the heat of formation of the reagents and products was used to calculate the theoretical energy consumption of the corresponding reactions and scaled up using industrial empirical factors reported in literature.[25] For example, the necessary heat in endothermic reactions was assumed to be supplied from natural gas and the theoretical energy requirements were multiplied by a factor of 4.2. In the case of electricity consumption for cooling down exothermic reactions, a factor of 3.2 was applied to the theoretical estimations. These estimations only include the direct consumption in the reactors, thus excluding contributions from other unit operations such as separations and pumping. However, this approach is considered to be appropriate for the purposes of this study as previous LCA studies of ILs have indicated that in most cases the large number of precursors, *i.e.* raw materials, are the main contributors to their environmental impacts.[46] The co-products were credited to the system, *e.g.* hydrochloric acid, sodium chloride and lithium chloride, and the organic waste was assumed to be treated in a wastewater treatment plant. All the background data for the raw materials, energy systems and waste management processes were sourced from the Ecoinvent database v3.8.[31] Ethylene dichloride was used as a proxy for butyl chloride, hexyl chloride, octyl chloride and decyl chloride production, and benzyl chloride was used as a proxy for phenyl chloride due to a lack of data for these chemicals in the Ecoinvent database.

2.3.3 Life cycle impact assessment. The LCA modelling was carried out using the LCA for Experts software,[47] and the environmental impacts were estimated with the CML-IA 2001: August 2016 impact assessment method.[48] The impact categories estimated in this study are GWP, human toxicity potential (HTP), freshwater aquatic ecotoxicity potential (FAETP), marine aquatic ecotoxicity potential (MAETP), and terrestrial ecotoxicity potential (TETP) as these are considered to have the strongest influence of choice in the IL when applied at scale.[49]

2.4 Group-contribution analysis and validation

The final stage of the methodology involves the group-contribution (GC) analysis and the development of predictive models for the environmental impacts of ionic liquids (ILs). Given that the environmental impacts of imidazole-based ILs were estimated based on the individual contributions of the synthesis steps described in Section 2.2 and Fig. 4, it is reasonable to employ a GC modelling approach. This allows for the correlation of environmental impacts with the functional chemical groups introduced during each synthesis step.

Hukkerikar *et al.*[33] reported a similar correlative approach to describe the environmental properties of organic molecules. In the present work, a group additivity method, similar to that of Benson and co-workers, was adopted.[50,51] In this framework,

Table 2 Raw materials, co-products and waste inventory for the production of 1 mol of imidazolium chloride ILs

Synthesis step	Reactants	Products, co-products and waste	Quantity (g per mol IL)									
			[Hmim]Cl	[C_2mim]Cl	[C_4mim]Cl	[C_6mim]Cl	[C_8mim]Cl	[C_{10}mim]Cl	[Amim]Cl	[Bzmim]Cl	[Phmim]Cl	[C_4dmim]Cl
Ring formation[a]	Glyoxal		88	88	88	88	88	88	88	88	88	88
	Ammonia		51	52	52	52	52	52	52	52	52	52
	Formaldehyde		45	46	46	46	46	46	46	46	46	—
	Acetaldehyde		—	—	—	—	—	—	—	—	—	67
		1*H*-Imidazole	87	88	88	88	88	88	88	88	88	—
		2-Methylimidazole	—	—	—	—	—	—	—	—	—	106
		Water	69	70	70	70	70	70	70	70	70	70
		Organic waste	28	28	28	28	28	28	28	28	28	31
Methylation[b]	1*H*-Imidazole		87	88	88	88	88	88	88	88	88	—
	2-Methylimidazole		—	—	—	—	—	—	—	—	—	106
	Methyl chloride		65	65	65	65	65	65	65	65	65	65
		1-Methylimidazole chloride[e]	**118.56**	—	—	—	—	—	—	—	—	—
		1-Methylimidazole	—	83	83	83	83	83	83	83	83	—
		1,2-Dimethylimidazole	—	—	—	—	—	—	—	—	—	97
		Hydrochloric acid	—	37	37	37	37	37	37	37	37	37
		Organic waste	33	34	34	34	34	34	34	34	34	38
Alkylation[c]	1-Methylimidazole		—	83	83	83	83	83	83	83	83	—
	1,2-Dimethylimidazole		—	—	—	—	—	—	—	—	—	97
	Ethyl chloride		—	85	—	—	—	—	—	—	—	—
	Butyl chloride[d]		—	—	122	—	—	—	—	—	—	122
	Hexyl chloride[d]		—	—	—	158	—	—	—	—	—	—
	Octyl chloride[d]						195				—	
	Decyl chloride[d]		—	—	—	—	—	232	—	—	—	—
	Allyl chloride		—	—	—	—	—	—	101	—	—	—
	Benzyl chloride		—	—	—	—	—	—	—	166	—	—
	Phenyl chloride[e]						—				148	
		Imidazolium chloride[f]	**—**	**146.56**	**174.67**	**202.72**	**231**	**258.83**	**158.63**	**208.69**	**195**	**188.7**
		Organic waste	—	21	30	39	47.4	56	25	41	36	30

[a] Reaction yield assumed at 85%.[36] [b] Reaction yield assumed at 76%.[37] [c] Reaction yield assumed at 99%.[40] [d] Ethylene dichloride was used as a proxy. [e] Benzyl chloride was used as a proxy.[f] Main IL product in grams and equivalent to 1 mol of IL.

Table 3 Raw materials, co-products and waste inventory for the production of 1 mol of imidazolium tetrafluoroborate ILs

Synthesis step	Reactants	Products, co-products and waste	Quantity (g per mol IL)										
			[Hmim][BF_4]	[C_2mim][BF_4]	[C_4mim][BF_4]	[C_6mim][BF_4]	[C_8mim][BF_4]	[C_{10}mim][BF_4]	[Amim][BF_4]	[Bzmim][BF_4]	[Phmim][BF_4]	[C_4dmim][BF_4]
Anion metathesis[a]	1-Methylimidazole chloride		130	—	—	—	—	—	—	—	—	—	—
	Imidazolium chloride		—	161	192	223	254	284	174	229	214	207	
	Sodium tetrafluoro-borate		121	121	121	121	121	121	121	121	121	121	
		Imidazolium tetrafluoroborate[b]	**168.9**	**198**	**226**	**254**	**282**	**310**	**210**	**260**	**246**	**240**	
		Sodium chloride	58	58	58	58	58	58	58	58	58	58	
		Organic waste	23	25	28	31	34	36	27	32	30	30	

[a] Reaction yield assumed at 91%.[41] [b] Main IL product in grams and equivalent to 1 mol of IL.

a group is defined as a polyvalent atom (or moiety) and its nearest neighbours, denoted as $X–(A)_i(B)_j(C)_k(D)_l$, where X is the central atom bonded to atoms A, B, C, and D with respective multiplicities i, j, k, and l.

Due to the limited number of cations and anions analysed in this study, only ten distinct groups were defined and used in the model. Nevertheless, this analysis demonstrates the feasibility of using GC models to estimate the environmental impacts of ILs, analogous to their widespread application for predicting physicochemical properties.[52,53] The chemical groups used are depicted in Fig. 5 and listed in Table S8 in the SI. As shown, certain groups (*e.g.*, methyl and methylene) recur frequently across multiple ILs, while others (*e.g.*, the phenyl group, $C_b–(C)\equiv C_b–(N)$ and the vinyl group, $C_v–(C)$) appear only once, limiting their transferability to ILs outside the current database.

The GC model proposed in this work is a linear model of the form

$$f = \sum_i n_i \beta_i \quad (1)$$

where f represents the environmental impact, β_i is the contribution group i, and n_i is the number of occurrences of group i in the molecule. Note that the intercept of the linear model is incorporated into the contribution of the imidazole group.

From the total of 30 ILs considered, 24 were randomly selected for model training and validation, while the remaining 6 were reserved as a test set to evaluate final model performance. The specific ILs assigned to training/validation, and testing are provided in Table S1 in the SI. Given the relatively small dataset, resampling techniques were applied to reduce overfitting and increase confidence in the models developed.[54–56] Specifically, k-fold cross-validation (CV) and bootstrap (BS) resampling methods were employed.

In k-fold CV, the dataset is split into k equally sized and randomly selected subsets. Each fold is used once for validation while the remaining $k-1$ folds are used to train the model (*i.e.*, estimate the coefficients β_i). This process is repeated k times, ensuring each fold has been used once as validation set, and the average root-mean-square error (RMSE) across the validation sets is used to evaluate performance. CV was performed for all divisors of 18, *i.e.*, $k = 2$, 3, 6, 9, and 18, the latter corresponding to the special case of leave-one-out CV (LOOCV). For the bootstrap sampling, 10^4 datasets of size 18 were generated by sampling with replacement. Model coefficients were estimated using each bootstrap sample, and the RMSE for each was calculated using the out-of-bag data.

An important aspect in the fitting of the models is the contribution of the imidazole group, denoted by C_{im}, which is common in all IL studied in this work. If not address, its contribution would artificially assigned a coefficient of zero during the optimization, with its actual effect distributed across other groups. To avoid this problem, model fitting was restricted to groups introduced *via* alkylation and anion metathesis reactions. The contribution of the imidazole group was computed separately as average of the sum of the ring formation and methylation contributions plus the intercept of the linear model and was not further optimised. After the model

Table 4 Raw materials, co-products and waste inventory for the production of 1 mol of imidazolium hexafluorophosphate ILs

Synthesis step	Reactants	Products, co-productsand waste	Quantity (g per mol IL)									
			[Hmim][PF_6]	[C_2mim][PF_6]	[C_4mim][PF_6]	[C_6mim][PF_6]	[C_8mim][PF_6]	[C_{10}mim][PF_6]	[Amim][PF_6]	[Bzmim][PF_6]	[Phmim][PF_6]	[C_4dmim][PF_6]
Anion metathesis[a]	1-Methylimidazole		130	—	—	—	—	—	—	—	—	—
	Imidazolium chloride		—	161	192	223	254	284	174	229	214	207
	Lithium hexafluoro-phosphate		121	167	167	167	167	167	167	167	167	167
		Imidazolium hexafluoro-phosphate[b]	228	256	284	312	340	368	268	318	304	298
		Lithium chloride	42	42	42	42	42	42	42	42	42	42
		Organic waste	27	30	32	35	38	41	31	36	35	34

[a] Reaction yield assumed at 91%.[41] [b] Main IL product in grams and equivalent to 1 mol of IL.

development, predictive accuracy was assessed using the six ILs reserved for testing.

3 Results and discussion

The results of the environmental impact of the ILs sample obtained from the LCA analysis are presented first, including a comparison with results of other ILs reported in the literature and conventional organic solvents. This is followed by the GC predictive models results and discussion.

3.1 Environmental impact assessment of ILs

The results of all imidazolium chloride ILs have been analysed first to focus on the contributions from the cationic part of the molecule, followed by the results for the imidazolium tetrafluoroborates and imidazolium hexafluorophosphates to look at the anion contributions. The GWP results are presented first, followed by HTP, FAETP, MAETP and TETP, which are presented in Section 3.1.2.

3.1.1 Global warming potential. The GWP results of all the imidazolium chloride ILs are presented in Fig. 6. The estimated total GWP for these ILs ranges from 0.73 kg CO_2 eq. per mol to 1.07 kg CO_2 eq. per mol. The formation of the imidazole ring is responsible for the majority of this impact, contributing between 44% and 63% of the total GWP mainly due to the use of glyoxal. In the particular case of [Hmim]Cl, the ring formation step contributes the highest (63%) impact because this IL only has one substituent and therefore, requires only two synthesis steps. This is also the reason why it has the lowest GWP (0.73 kg CO_2 eq. per mol), as it requires fewer reagents overall.

It can also be observed in Fig. 6 that the GWP of the ring formation step for IL [C_4dmim]Cl is the second largest, contributing to 59% of the total impact. This is because of the use of acetaldehyde instead of formaldehyde, which is needed to obtain the three alkyl substituents.

The GWP of the methylation step is estimated around 0.19 kg of CO_2 eq. per mol for all imidazolium chloride ILs under study, as this step is the same across all ILs, *i.e.* all precursors react with methyl chloride to produce 1-methylimidazole or 1,2-dimethyilimidazole in the case of [C_4dmim]Cl. Consequently, the slight variations between these values are due to yield differences and corresponding energy requirements. This step contributes between 17% and 37% of the total GWP impact, and the use of methyl chloride is responsible for the significant contributions from this synthesis step.

With the exception of [Hmim]Cl, the alkylation step is the second hotspot for all ILs and contributes with 21% to 39% of the total GWP results. It can be inferred that the magnitude of the environmental impacts of the imidazolium chloride ILs studied here, will depend on the alkylation step as each IL will require a specific alkyl halide, which in turn will have different environmental burdens depending on their production, *e.g.* length of alkyl chain, presence of aromatics. For example, [C_{10}mim]Cl, [Phmin]Cl and [Bzmim]Cl have the highest GWP reported at 0.99 kg CO_2 eq. per mol, 1.02 kg CO_2 eq. per mol and 1.07 kg CO_2 eq. per mol, respectively, mainly because of the

Table 5 Energy consumption data for the production of 1 mol of imidazolium based ILs

		Quantity (MJ per mol IL)									
Synthesis step	Type of energy[c]	[Hmim]Cl	[C_2mim]Cl	[C_4mim]Cl	[C_6mim]Cl	[C_8mim]Cl	[C_{10}mim]Cl	[Amim]Cl	[Bzmim]Cl	[Phmim]Cl	[C_4dmim]Cl
Ring formation	Cooling	1.58	1.73	1.73	1.73	1.57	1.73	1.73	1.73	1.57	1.60
Methylation	Heating	1.26	—	—	—	—	—	—	—	—	0.03
	Cooling	—	0.16	0.16	0.16	0.15	0.16	0.16	0.16	0.15	—
Alkylation	Heating	—	1.77	1.95	1.90	2.12	2.16	1.21	1.29	1.12	1.95
Anion metathesis $[BF_4]^-$[a]	Heating	6.00	6.00	6.00	6.00	6.00	6.00	6.00	6.00	6.00	6.00
Anion metathesis $[PF_6]^-$[b]	Heating	8.00	8.00	8.00	8.00	8.00	8.00	8.00	8.00	8.00	8.00

[a] Imidazolium tetrafluoroborate ionic liquids. [b] Imidazolium hexafluorophosphate ionic liquids. [c] Scaled-up energy consumption.

longest alkyl chain and aromatic groups considered in their alkylation steps. It should be noted that while ethylene dichloride was used as a proxy for most alkyl halide precursors due to limited data in the Ecoinvent database, the quantities required were calculated using stoichiometric relationships specific to each ionic liquid synthesis pathway. This ensures that differences in raw material requirements for each IL are reflected as closely as possible, within the limitations of the available data, in the environmental impact estimations. [C_2mim]Cl, on the other hand, has a total GWP of 0.83 kg CO_2 eq. per mol as it used ethyl chloride (the shortest alkyl chain considered). Therefore, the side chain variations obtained during the alkylation step can potentially be considered the most influential step in the overall GWP of imidazolium based ILs.

The effect that the number of substituents on the imidazole ring has on the GWP of imidazole-based ILs was also studied using [C_4mim]Cl and [C_4dmim]Cl as an example, as they have two and three substituents, respectively. In addition, both ILs use the same alkyl halide (butyl chloride) in the alkylation step. The GWP results for these ILs are estimated at 0.87 kg CO_2 eq. per mol and 0.94 kg CO_2 eq. per mol, respectively. This difference is mainly due to the use of formaldehyde and acetaldehyde in the ring formation step, as the number of substituents plays a negligible effect in the overall GW of these two ILs. It was also observed that the presence of a double bond in any of the side chains does not seem to influence the GWP of the ILs. For example, the GWP of [Amim]Cl, which contains a three-carbon unsaturated substituent, is estimated at 0.83 kg CO_2 eq. per mol, which is same to the GWP results estimated for [C_2mim]Cl and close to [C_4mim]Cl estimated at 0.87 kg CO_2 eq. per mol, which have a two and four carbon saturated substituents, respectively.

The contributions from the anion exchange step are shown in Fig. 6 for both the $[BF_4]^-$ and $[PF_6]^-$ anions. The imidazolium chloride ILs are the precursors for the preparation of the corresponding imidazolium tetrafluoroborate and imidazolium hexafluorophosphate ILs shown in Fig. 6. According to these results, the GWP of the resulting ILs is approximately 2.7 and 4.8 times higher when substituting the chloride anion with $[BF_4]^-$ and $[PF_6]^-$, respectively. This is because an equimolar amount of salt (with respect to the imidazolium chloride precursor) is required in the anion metathesis step, and these anions are assumed to be derived from salts with considerably high carbon footprints. For example, the GWP of sodium tetrafluoroborate and lithium hexafluorophosphate salts are reported at 10.3 kg CO_2 eq. per kg and 19.3 kg CO_2 eq. per kg, respectively.[57] The contributions from this step will largely depend on the environmental burdens of the metal salts or other chemicals used to obtain the desired anions. Therefore, given the great influence this step has over the total GWP impact of imidazole ILs, special consideration should be given to the selection and sourcing of the anion. The use of LCA databases can help when considering the latter.

3.1.2 Human toxicity impacts. The results for the human toxicity potential (HTP) impact category for all ILs are presented in Fig. 7. The HTP results of the imidazolium-chloride ILs are

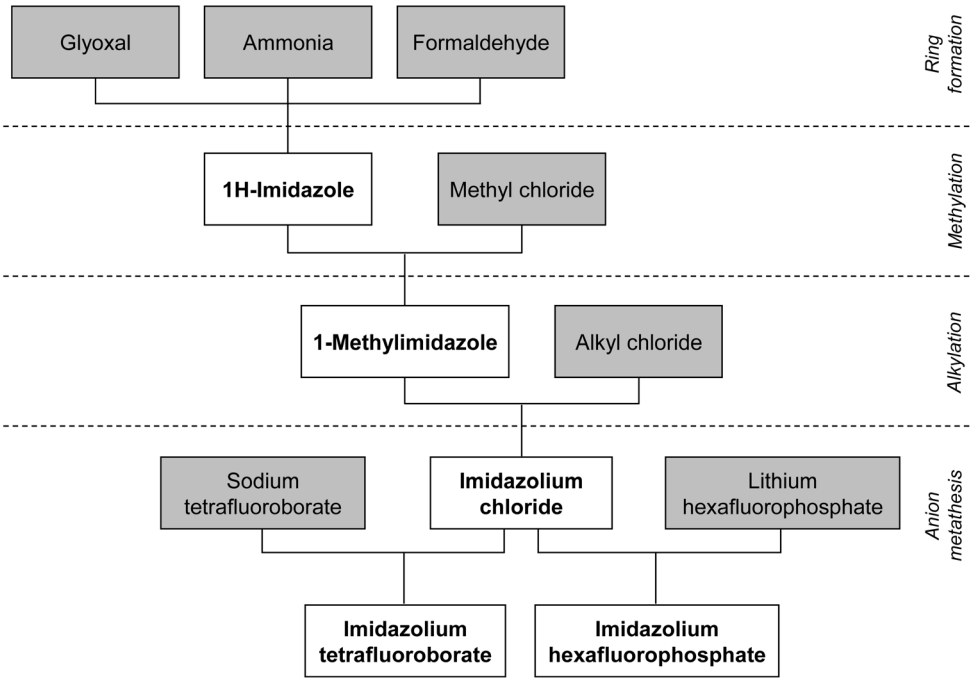

Fig. 4 Generic life cycle tree for the production of alkyl imidazolium [the shaded boxes indicate the compounds for which data are available in the Ecoinvent database.[27] Data for the compounds shown in white boxes are not currently available].

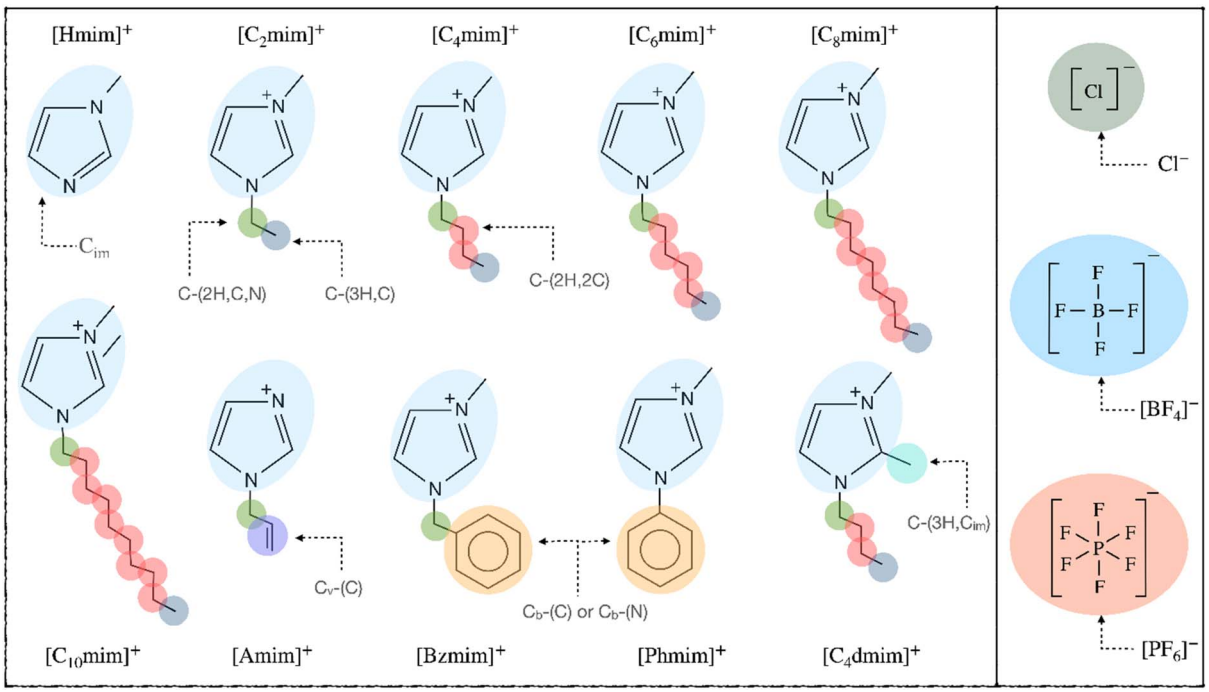

Fig. 5 Chemical groups used for the development of the GC models. The names of the 10 groups analysed are also indicated.

estimated at around 6 kg DCB eq. per mol of IL. The formation of the imidazole ring is the dominating synthesis step under this category as it contributes with over 98% of the total impact, whilst contributions from the alkylation step are negligible. This is due to the production of glyoxal *via* the oxidation of ethylene oxide, as it releases toxic emissions of ethylene oxide to water and air, a well-known genotoxic substance.[58] The glyoxal production process in Ecoinvent (RER: glyoxal production) assumes the release of 0.2% of fugitive emissions of ethylene oxide to the atmosphere in the absence of process emissions in

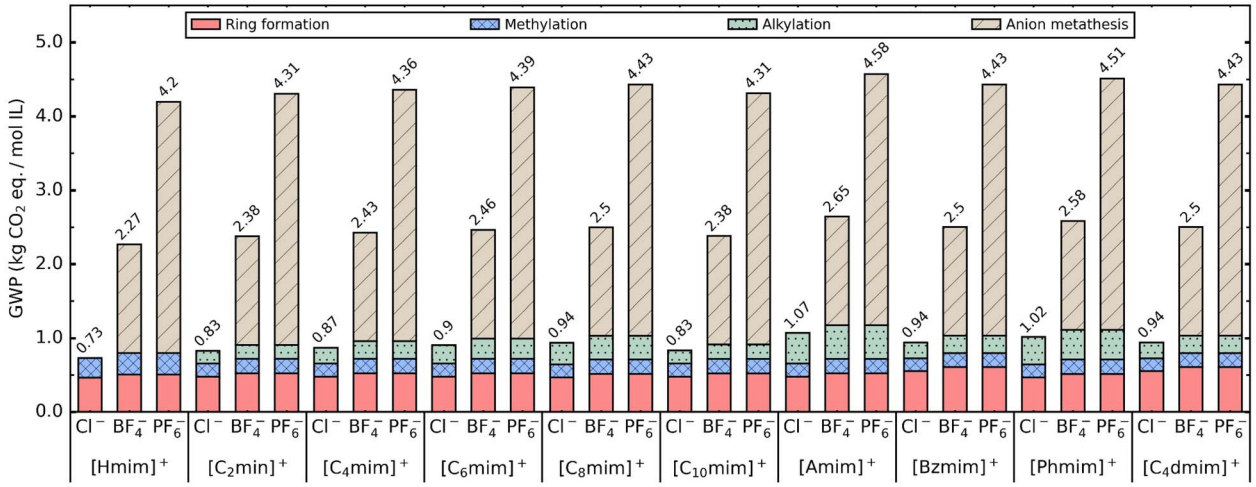

Fig. 6 Global warming potential (GWP) of imidazolium chloride, imidazolium tetrafluoroborate and imidazolium hexafluorophosphate ILs, showing synthesis steps contributions [1-methylimidazolium ($[Hmim]^+$); 1-ethyl-3-methylimidazolium ($[C_2mim]^+$); 1-butyl-3-methylimidazolium ($[C_4mim]^+$); 1-hexyl-3-methylimidazolium ($[C_6mim]^+$); 1-octyl-3- methylimidazolium ($[C_8min]^+$), 1-decyl-3-methylimidazolium ($[C_{10}mim]^+$); 1-allyl-3-methylimidazolium ($[Amim]^+$); 1-benzyl-3-methylimidazolium ($[Bzmim]^+$); 1-phenyl-3-methylimidazolium ($[Phmin]^+$); 1-butyl-2,3-dimethylimidazolium ($[C_4dmim]^+$); chloride (Cl^-); tetrafluoroborate (BF_4^-); hexafluorophosphate (PF_6^-)].

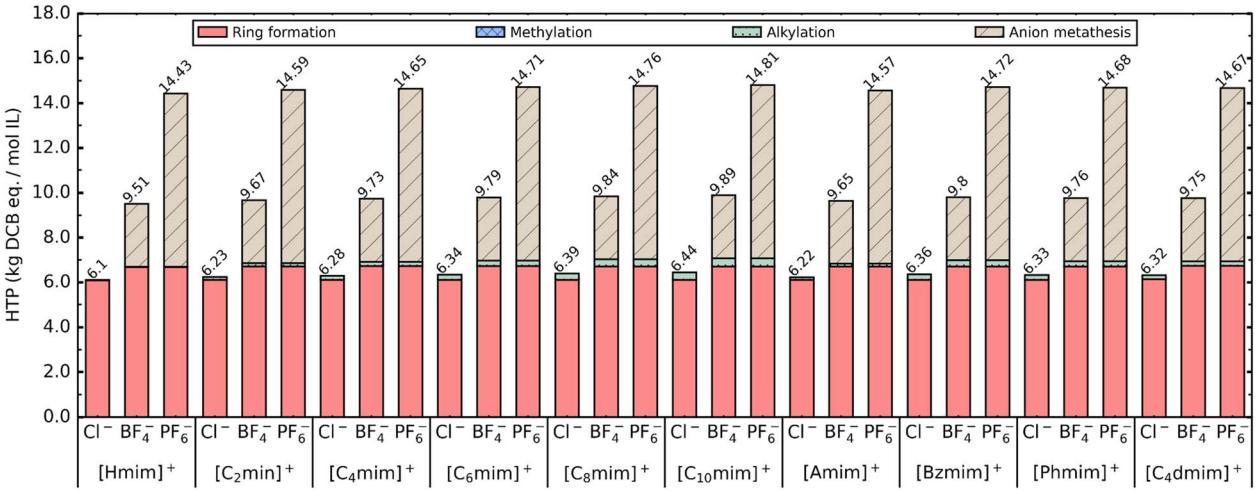

Fig. 7 Human toxicity potential (HTP) impacts of imidazolium chloride, imidazolium tetrafluoroborate and imidazolium hexafluorophosphate ILs, showing synthesis steps contributions [for the ILs names, see Table 1 and Fig. 6].

the literature.[57] However, this value is extremely high compared to fugitive emissions considered in other relevant industrial processes in the database. For example, the processes for ethylene oxide and ethylene glycol are reported to emit 0.002% and 0.0006% of ethylene oxide per kg produced, respectively.[57]

In the CML-IA 2001: August 2016 method, HTP, as well as ecotoxicities potentials, are calculated with an adapted Uniform System for the Evaluation of Substances model for LCA known as the USES-LCA model. The model describes the fate, exposure and effects of toxic substances in various environmental media for an infinite time horizon, and the database contains toxicity data for over 3300 chemicals for a large number of species.[59] In terms of spatial differentiation, the USES-LCA model takes a site-generic approach, *i.e.* generic receiving environments as opposed to region or source specific environments. Each toxic substance is assigned a characterisation factor with respect to 1,4-dicholorobenzene (DCB), which is the reference substance assigned for all toxicity impacts in the CML-AI 2001: August 2016 method. In the case of ethylene oxide, this is 14 075 kg DCB equivalent per kg of emission, thus resulting in such a high contribution.[60] The infinite time horizon and the spatial differentiation approach have been identified as limitations to the accuracy of the USES-LCA model, and other models such as USEtox have become widely accepted.[61]

The ring formation is also the main hotspot in HTP for imidazolium tetrafluoroborate ILs (69%) and the second hotspot for imidazolium hexafluorophosphate ILs (47%), as shown in Fig. 7. For imidazolium hexafluorophosphate ILs, the use of

lithium hexafluorophosphate salts accounts for around 52% of this impact, thus identified as the main hotspot. Similar to GWP, $[PF_6]^-$ anion causes higher impacts under this impact category because of the release of hydrogen fluoride emissions during its preparation, which is known for its severe toxic effects to human health.[62] This intrinsic toxicity of lithium hexafluorophosphate is increased by the fact that this salt has a higher molecular weight and must therefore be used in greater quantities than the respective tetrafluoroborate salt. Therefore resulting in HTP results 2 times higher compared to their corresponding imidazolium chloride counterpart.

3.1.3 Ecotoxicity impacts. The ecotoxicity impact results for all ILs are presented in Fig. 8–10. The freshwater aquatic ecotoxicity potential (FAETP) and marine aquatic ecotoxicity potential (MAETP) results are presented in Fig. 8 and 9, and are estimated at 0.2–0.3 kg DCB eq. per mol and 0.4–0.6 t DCB eq. per mol, respectively for all imidazolium-chloride ILs. Very similar trends can be observed for FAETP and MAETP, where the ring formation is the predominant step, contributing between 54–95% and 50–87% of the total impacts of the ILs, respectively. The alkylation step contributes 29–53%, depending on the length of the chain. For example, ethyl chloride and decyl chloride used in the preparation of $[C_2mim]Cl$ and $[C_{10}mim]Cl$ have the lowest and highest contributions, respectively. The methylation step, on the other hand, causes a negligible effect under these impact categories. This is because of the co-production of hydrochloric acid, which is credited to the system and therefore showing a net-negative impact in the case of FAETP and minimal contribution for MAETP. In the case of [Hmim]Cl, the ring formation step contributes >87% of the impacts as there is no alkylation step and the contributions from the methylation step are negligible as previously explained.

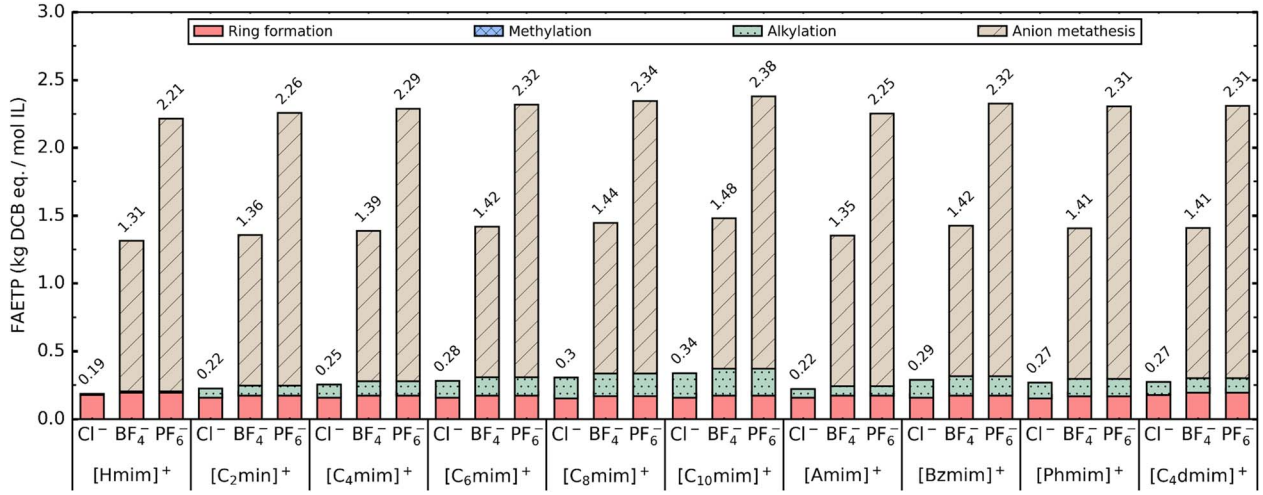

Fig. 8 Freshwater aquatic ecotoxicity potential (FAETP) impacts of imidazolium chloride, imidazolium tetrafluoroborate and imidazolium hexafluorophosphate ILs, showing synthesis steps contributions [for the ILs names, see Table 1 and Fig. 6].

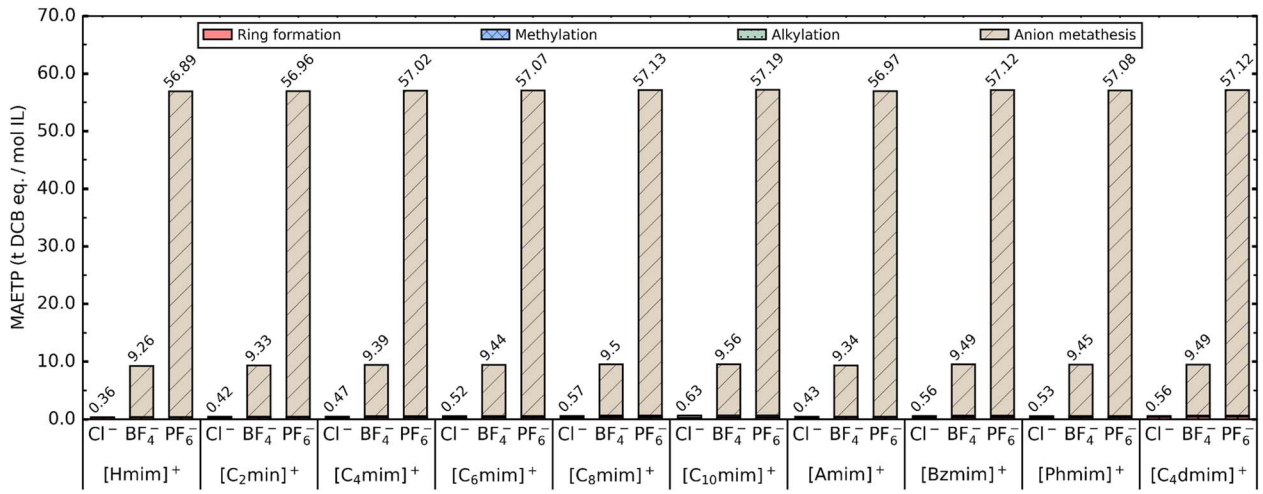

Fig. 9 Marine aquatic ecotoxicity (MAETP) impacts of imidazolium chloride, imidazolium tetrafluoroborate and imidazolium hexafluorophosphate ILs, showing synthesis steps contributions [for the ILs names, see Table 1 and Fig. 6].

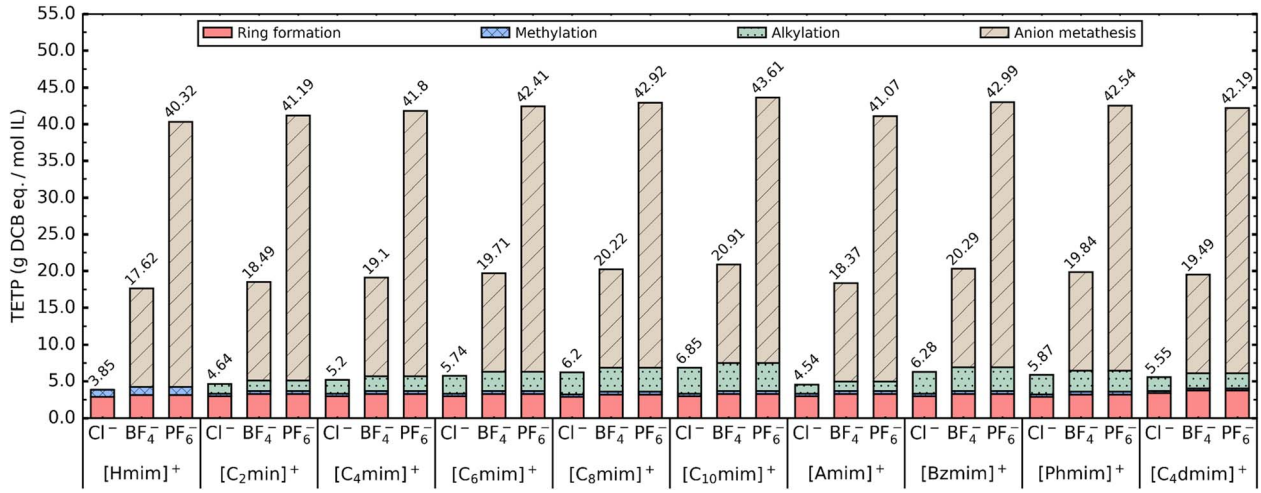

Fig. 10 Terrestrial ecotoxicity potential (TETP) impacts of imidazolium chloride, imidazolium tetrafluoroborate and imidazolium hexafluorophosphate ILs, showing synthesis steps contributions [for the ILs names, see Table 1 and Fig. 6].

Fig. 10 presents the terrestrial ecotoxicity potential (TETP) results of the studied imidazolium chloride ILs, and this is calculated between 3.85 g DCB eq. per mol and 6.85 g DCB eq. per mol. As it can be observed, the ring formation step contributes with 52–74% of the total impact mainly due to the glyoxal production. This is followed by the alkylation step, with contributions between 28–51% of the total impact. The toxicity results presented in this section also indicate that the use of alkylation agents with longer alkyl chains or aromatic groups will cause higher contributions to the overall toxicity of the IL. In this case, it is observed that the use of decyl chloride and benzyl chloride causes the highest contributions among all toxicity impact categories.

In the case of the imidazolium tetrafluoroborate and imidazolium hexafluorophosphate ILs, the results show that the total impact results for FAETP, MAETP and TETP are predominantly driven by the anion metathesis reaction due to the choice of anion. The use of sodium tetrafluoroborate and lithium hexafluorophosphate salts causes significant increases to the total ecotoxicity impacts of the ILs as in the case of GWP. For example, the impact results of imidazolium tetrafluoroborate ILs for TETP, FAETP and MAETP are around 3, 5 and 19 times higher compared to their corresponding imidazolium chloride counterpart, respectively. For the imidazolium hexafluorophosphate ILs, these are approximately 7, 9 and 116 times higher. Similar to GWP and HTP, the $[PF_6]^-$ anion causes higher environmental impacts across all ecotoxicity impact categories.

3.1.4 Comparisons with other ILs and conventional organic solvents. In this section, the environmental impact results of [Hmim]Cl, [C_4mim]Cl, and [C_4mim][BF_4] estimated in this study, were compared on a mass basis (kg CO_2 eq. per kg IL) with other similar ILs reported in the literature for validation purposes,[22,24,26,27,29,30] and with a selection of commonly used conventional organic solvents in industry[63] for reference. Comparisons were only possible between studies reporting midpoint indicators estimated using compatible impact assessment methods. The group of conventional solvents comprises 16 different solvents across the following categories: alcohols, aliphatic hydrocarbons, amines, aromatic hydrocarbons, esters, ethers, halogenated solvents, ketones and sulfur containing solvents. The full list of solvents is included in Table S7 in the SI, including the specific Ecoinvent processes used to calculate their environmental impacts.[31] The GWP impact results are presented in Fig. 11.

Baaqel *et al.*[26] reported the GWP impact for [Hmim][HSO_4], which was estimated at 2.7 kg CO_2 eq. per kg IL, which is 55% lower compared to [Hmim]Cl assessed in this study, as shown in Fig. 11. Such differences can be attributed to the fact that the IL [Hmim][HSO_4] is assumed to be synthesized *via* the transfer of a proton from a Brønsted acid (sulfuric acid) to a Brønsted base (1-methylimidazole),[26] has a different non-halogenated anion, and the inventory data was obtained from a process simulation based on a scaled-up manufacturing process from literature.[64] However, both studies assumed that 1-methylimidazole was synthesized using the Debus–Radziszewski method hence using the same precursors for this stage.

Righi *et al.*[24] and Amado Alviz and Alvarez[30] assessed the environmental impacts of halogenated ILs [C_4mim]Cl and [C_4mim]Br, respectively, which also considered their preparation *via* the alkylation and salt metathesis route. The results of these studies are comparable and GWP impact of these ILs ranges between 5.9–6.4 kg CO_2 eq. per kg IL. Zhang *et al.*[27] reported a GWP impact of 3.5 kg CO_2 eq. per kg IL for [C_4mim][BF_4], which is 67% lower compared to the one estimated in this study, even though both studies have assumed the same preparation method and the use of the same precursors. However, due to a lack of further information it is not possible to explain the observed differences. Cuéllar-Franca *et al.*[22] reported the GWP of 1-butyl-3-methylimidazolium acetate ([C_4mim][Oac]) at 7.4 kg CO_2 eq. per kg IL and 1-butyl-3-methylimidazolium sulfate ([C_4mim][H_2SO_4]) at 4.4 kg CO_2 eq. per kg IL, which are 30% and 58% lower compared to [C_4mim][BF_4] studied here,

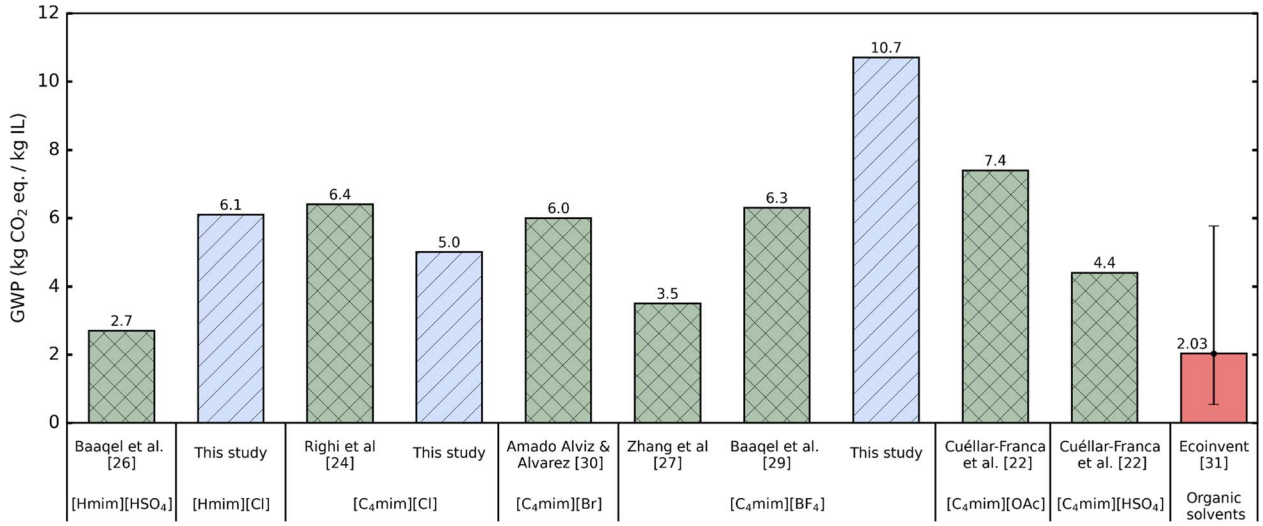

Fig. 11 Comparison of global warming potential (GWP) per kg of imidazolium-based ionic liquids estimated in this study with literature values for different synthesis routes and conventional organic solvents[22,24,26,27,29–31] [the average GW impact of 16 solvents from different categories is presented here; the error bars indicate the maximum and minimum GW reported for the solvents. The full list of solvents and corresponding GW impacts can be found in Table S7].

as shown in Fig. 11. These ILs were assumed to be prepared *via* a halide free route, which can explain the variations observed.

A more recent study by Baaqel *et al.*[29] compared two synthesis routes for the preparation of $[C_4mim][BF_4]$, a one-pot halide-free and an alkylation and salt metathesis routes. The results indicate a significantly lower GWP for the halide-free route (6.3 kg CO_2 eq. per kg solvent), corresponding to a 78% reduction compared to the metathesis route. Although the GWP results reported for the metathesis route (27.26 kg CO_2 eq. per kg solvent) is much higher than that estimated in this study for the same IL (10.7 kg CO_2 eq. per kg solvent), largely due to the use of sodium tetrafluoro-borate salt in excess, these results are consistent with an emerging indication that halide-free routes may be associated with lower GWP values than alkylation and salt metathesis routes.

The average GWP impact of the organic solvents presented in Fig. 11 is 2.03 kg CO_2 eq. per kg solvent, which is 65% lower compared to the average GWP of the ILs discussed in this section. Methanol and hexane are among the solvents with the lowest GWP, with an average of 0.57 kg CO_2 eq. per kg, whilst propylene glycol, monoethanolamine and ethylene bromide have the highest GWP of the selected solvents, with an average of 4.2 kg CO_2 eq. per kg. The halogenated solvent is comparable to most ILs presented in Fig. 11. Several organic solvents such as hexane are obtained from petroleum mixtures through a series of separation steps, thus resulting in lower GWP impacts compared to solvents that required several energy intensive reaction and separation steps for their production, and the use of numerous precursors.

3.2 Group contribution analysis and predictive models

The results of the GC models developed for the environmental impacts of the 30 ILs studied, specifically for GWP, HTP, FAETP, MAETP, and TETP, are presented in Fig. 12.

The average RMSE obtained through both *k*-fold CV and BS resampling is shown in Fig. 12. For CV, the average RMSE exhibits minimal variation with the number of folds; however, a slight decreasing trend is observed as the value of *k* increases. The lowest RMSE values are achieved at $k = 18$, corresponding to the LOOCV leave limit. The only exception is HTP, where the RMSE remains nearly constant across all *k* values. This stability is attributed to the dominant and consistent contributions of the ring formation and anion metathesis steps, with minimal variation from the alkylation step.

The RMSE values obtained *via* BS sampling are slightly higher than those from LOOCV, but remain comparable to the RMSE values from *k*-fold CV. The overall consistency across all resampling techniques confirms the robustness and reliability of the GC models. In all cases, the low RMSE values indicate strong model performance and excellent agreement with the underlying LCA data.

To demonstrate the predictive capability of the models, results from LOOCV are used exclusively for generating parity plots, shown in Fig. 12(b–f). These plots compare the predicted environmental impacts against the corresponding values obtained directly from LCA. Overall, the models show excellent agreement with the LCA data for both the training and test sets, supporting their generalizability and predictive accuracy.

As discussed earlier, the data naturally cluster into three distinct regions based on the anion used in the IL: $Cl^- < [BF_4]^- < [PF_6]^-$. This clustering effect is especially pronounced in the MAETP results, where the anion metathesis step accounts for over 92% of the total impact. Insets in each plot highlight the Cl^--based ILs to reveal the finer variations arising from the functional groups in the cation. These differences illustrate the sensitivity of the GC model to structural variations within the cation.

With the exception of HTP, which consistently deviates from the parity line due to systematic over- or underestimation, the

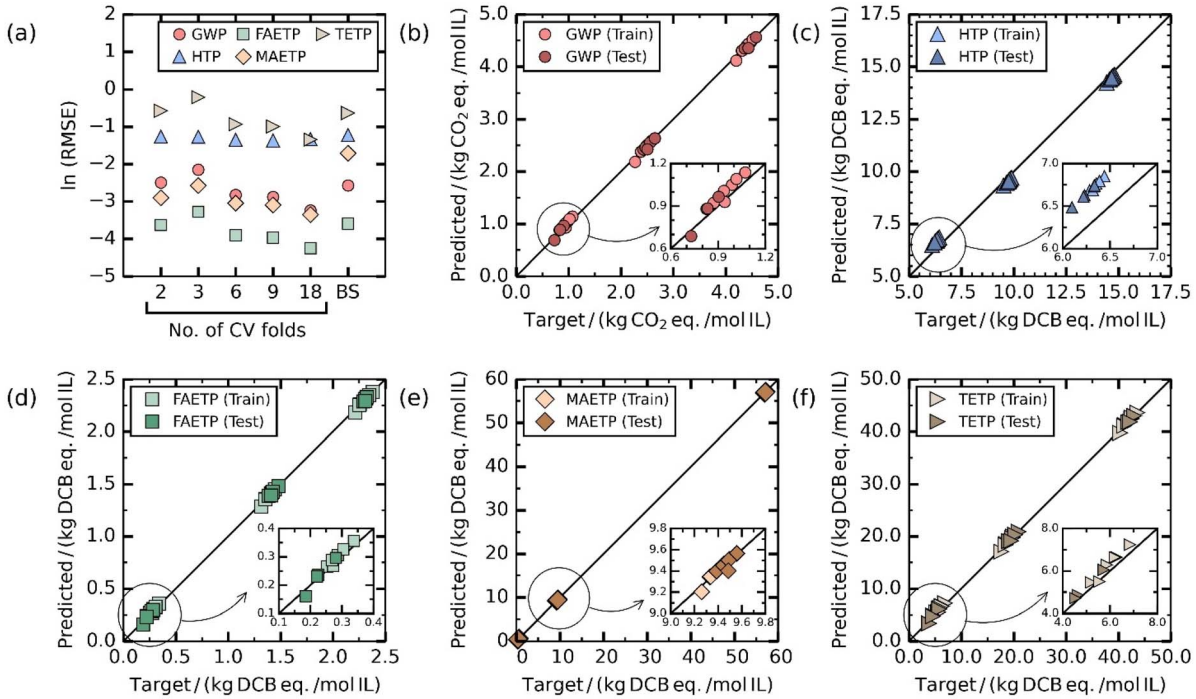

Fig. 12 Results of the group-contribution model proposed in this study to calculate environmental impacts using the linear model given by eqn (1) [(a) the results for the root-mean-square error (RMSE) as a function of the number of folds used in the cross-validation analysis are presented for all environmental impacts. The RMSE obtained from the bootstrap sampling is also shown (set BS). (b)–(f) are the parity plots representing the target and predicted environmental impacts using our GC model with the model obtained from LOOCV. The symbols with light shades represent the results for the 18 ILs used for training and validation, while the darker shades represent the predictions for the test set. The results correspond to (b) global warming potential (GWP), (c) human toxicity potential (HTP), (d) freshwater aquatic ecotoxicity potential (FAETP), (e) marine aquatic ecotoxicity potential (MAETP), and (f) terrestrial ecotoxicity potential (TETP)].

model predictions for all other impact categories align closely with the 1 : 1 diagonal, further confirming model accuracy. The deviation in HTP is attributed to contribution to the ring formation, which shows a variation between 6.1 and 6.8 kg DCB eq. per mol across all ILs studied, but this contribution in the GC model is represented by the average value of 6.5 kg DCB eq. per mol, which introduces a systematic error.

As previously noted, caution should be exercised when interpreting the contributions of chemical groups with limited representation in the dataset, particularly the vinyl and phenyl groups, which appear in only one IL each. While these groups were necessary for model completeness, their coefficients may be less reliable due to insufficient data for robust estimation. A sample calculation demonstrating the application of the predictive models is provided in the SI (see Table S9).

Nonetheless, the results clearly demonstrate the viability of using a GC-based approach to estimate the environmental impacts of ILs. Future work will expand the model to encompass a broader range of ILs, enhancing its predictive capabilities and enabling its use as a practical tool for early-stage design and screening of environmentally preferable ionic liquids.

3.3 Limitations and recommendations for future work

It is important to note that the predictive models developed in this study were based on a small sample size, and several limitations should be addressed in future work to fully evaluate the robustness of the models and increase the practical value of this research. For instance, expanding the sample of imidazolium-based ILs would improve the transferability of underrepresented chemical groups, such as phenyl and vinyl groups as well as other commonly used and relatively environmentally benign anions, *e.g.* derived from GRAS-listed substances such as acetates from acetic acid. The models should also be expanded to include other scalable synthesis methods for imidazolium-based ILs, including halide-free approaches, to systematically examine whether the emerging tendencies suggested by existing LCA studies are robust within the same IL family. These limitations can be addressed by systematically conducting LCAs across a broader range of ILs. However, it is recommended that frameworks combining process simulation and machine learning be used to generate the required volume of life cycle inventories. Examples of such approaches include those proposed by Martínez-Ramón *et al.*[65] and Baaqel *et al.*[28,66] Extending beyond imidazolium ILs, there is also a need to broaden the environmental impact evaluations to include other families of ionic liquids, particularly bio-based ILs, *e.g.* cholinium ILs, as well as other alternative solvents such as molten salts, deep eutectic solvents and natural deep eutectic solvents to understand how these approaches translate to other widely researched systems.

The environmental impacts data used to construct the predictive models excluded contributions from purification and

drying steps, which are typically required to remove impurities and excess water content. Purification and drying methods reported in the literature vary widely, ranging from simple techniques such as distillation, liquid–liquid extraction and filtration,[67,68] to more complex and expensive ones including vacuum distillation,[26,66] depending on the synthesis route and intended application. Although this exclusion represents a limitation of this work, since the contributions from these steps are unlikely to be negligible due to the use of solvents and utilities, selecting a specific purification technique without a defined application would be arbitrary and would introduce additional uncertainty into models intended for early-stage screening. Future work should therefore evaluate multiple purification and drying strategies feasible at commercial scales, both to quantify their potential impacts and to provide a framework for incorporating these contributions into predictive models. Such an approach would enable a more comprehensive assessment of the environmental impacts associated with ILs synthesis and support the development of robust guidelines and recommendations for their environmentally sustainable production. In principle, the contribution of a given purification step could be incorporated into the specific reaction step to which it is associated.

4 Conclusions

This study demonstrated that it is possible to correlate chemical functional groups and environmental properties such as global warming, human toxicity and eco-toxicity impacts of imidazolium-based ILs using linear models. An essential part of this work consisted in the estimation of the environmental impacts of a sample of 30 different imidazolium-based ILs using the LCA methodology, which included different cationic side chain substituents and types of connections, *e.g.* branching, double bonds, and the commonly used anions Cl^-, $[BF_4]^-$ and $[PF_6]^-$. The LCA results indicated that the choice of anion has a large influence over the environmental impacts of imidazolium-based ILs in the order $Cl^- < BF_4^- < PF_6^-$. The clear segregation was also evident in the linear predictive GC models that were developed as part of this work, demonstrating high accuracy according to the parity plots obtained.

For the imidazolium-chloride ILs, the ring formation steps was identified as the main hotspot for most impacts, followed by the alkylation step, which was a determining factor in the differences observed across the impacts of the ten ILs, whilst the presence of double bonds in the alkyl chain and the number of substituents on the imidazole ring had little influence over the environmental impacts of these ILs. For the imidazolium tetrafluoroborate and imidazolium hexafluorophosphate ILs, the anion metathesis step contributed significantly to all impact categories. Such high contribution was largely due to the environmental burdens associated with the use of sodium tetrafluoroborate and lithium hexafluorophosphate salts.

This work provides insights into opportunities for improving the design and synthesis of imidazolium-based ILs. The predictive environmental impact values obtained using the models proposed in this study should be regarded as indicative and interpreted within the scope, synthesis routes considered and limitations. Access to these data can support and facilitate more comprehensive life cycle assessments of ionic-liquid-based applications, *i.e.* cradle-to-grave, helping to make such studies accessible during the development of more sustainable applications. Detailed evaluations of ionic-liquid-based applications remain necessary on a case-by-case basis to fully understand the environmental sustainability of ILs, including both strengths and limitations, and to drive sustainable innovation across diverse applications.

Author contributions

Mirco Volanti: investigation and formal analysis of the LCA work, writing – original draft. Piya Gosalvitr: investigation and formal analysis of the LCA work. Carlos Avendaño: conceptualization, investigation and formal analysis of the group contribution work, writing – original draft, review & editing. Adam J. Greer: methodology guidance on selection of ILs sample and synthesis pathways, writing – review & editing. Christopher Hardacre: conceptualization and methodology guidance on selection of ILs sample and synthesis pathways, writing – review & editing. Fabrizio Passarini: conceptualization, supervision of Mirco Volanti, writing – review & editing. Rosa M. Cuéllar-Franca: conceptualization, investigation and formal analysis of the LCA work, writing – original draft, review & editing.

Conflicts of interest

There are no conflicts to declare.

Data availability

The data supporting this article have been included as part of the supplementary information (SI). Supplementary information is available. See DOI: https://doi.org/10.1039/d5su00658a.

References

1 Z. Lei, B. Chen, Y. M. Koo and D. R. MacFarlane, *Chem. Rev.*, 2017, **117**, 6633–6635.
2 A. J. Greer, J. Jacquemin and C. Hardacre, *Molecules*, 2020, **25**, 5207.
3 Z. Zhang, J. Song and B. Han, *Chem. Rev.*, 2017, **117**, 6834–6880.
4 S. F. R. Taylor, C. McCrellis, C. McStay, J. Jacquemin, C. Hardacre, M. Mercy, R. G. Bell and N. H. de Leeuw, *J. Solution Chem.*, 2015, **44**, 511–527.
5 A. J. Greer, S. F. R. Taylor, H. Daly, M. Quesne, C. R. A. Catlow, J. Jacquemin and C. Hardacre, *ACS Sustain. Chem. Eng.*, 2019, **7**, 3567–3574.
6 S. F. R. Taylor, M. McClung, C. McReynolds, H. Daly, A. J. Greer, J. Jacquemin and C. Hardacre, *Ind. Eng. Chem. Res.*, 2018, **57**, 17033–17042.

7 A. J. Greer, S. F. R. Taylor, H. Daly, M. G. Quesne, N. H. de Leeuw, C. R. A. Catlow, J. Jacquemin and C. Hardacre, *ACS Sustain. Chem. Eng.*, 2021, **9**, 7578–7586.
8 M. Watanabe, M. L. Thomas, S. Zhang, K. Ueno, T. Yasuda and K. Dokko, *Chem. Rev.*, 2017, **117**, 7190–7239.
9 N. V. Plechkova and K. R. Seddon, *Chem. Soc. Rev.*, 2008, **37**, 123–150.
10 M. B. Shiflett, J. W. Magee and D. Tuma, in *Commercial Applications of Ionic Liquids*, ed. M. B. Shiflett, Springer Cham, 2020, pp. 3–29.
11 R. S. Kalb, in *Commercial Applications of Ionic Liquids*, ed. M. B. Shiflett, Springer Cham, 2020, pp. 261–282.
12 A. R. Abouelela, F. V. Gschwend, F. Malaret and J. P. Hallett, in *Commercial Applications of Ionic Liquids*, ed. M. B. Shiflett, Springer Cham, 2020, pp. 87–127.
13 P. Berton, N. Abidi and J. L. Shamshina, *Curr. Opin. Green Sustainable Chem.*, 2022, **35**, 100625.
14 S. Koutsoukos, F. Philippi, F. Malaret and T. Welton, *Chem. Sci.*, 2021, **12**, 6820–6843.
15 D. Frenkel, B. Smit and B. Smit, *Understanding Molecular Simulation: from Algorithms to Applications*, Elsevier Science & Technology, San Diego, United States, 2001.
16 M. P. Allen and D. J. Tildesley, *Computer Simulation of Liquids*, Oxford University Press, Oxford, UK, 2nd edn, 2017.
17 V. Papaioannou, T. Lafitte, C. Avendaño, C. S. Adjiman, G. Jackson, E. A. Müller and A. Galindo, *J. Chem. Phys.*, 2014, **140**, 054107.
18 N. Abramenko, L. Kustov, L. Metelytsia, V. Kovalishyn, I. Tetko and W. Peijnenburg, *J. Hazard. Mater.*, 2020, **384**, 121429.
19 R. Gani, *Curr. Opin. Chem. Eng.*, 2019, **23**, 184–196.
20 B. E. Poling, J. M. Prausnitz and J. P. O'Connell, *The Properties of Gases and Liquids*, McGraw-Hill, United States, 5th edn, 2000.
21 Y. Chen, G. M. Kontogeorgis and J. M. Woodley, *Ind. Eng. Chem. Res.*, 2019, **58**, 4277–4292.
22 R. M. Cuéllar-Franca, P. García-Gutiérrez, J. P. Hallett and N. Mac Dowell, *React. Chem. Eng.*, 2021, **6**, 258–278.
23 R. M. Cuéllar-Franca, P. García-Gutiérrez, S. F. R. Taylor, C. Hardacre and A. Azapagic, *Faraday Discuss.*, 2016, **192**, 283–301.
24 S. Righi, A. Morfino, P. Galletti, C. Samorì, A. Tugnoli and C. Stramigioli, *Green Chem.*, 2011, **13**, 367–375.
25 A. Mehrkesh and A. T. Karunanithi, *ACS Sustain. Chem. Eng.*, 2013, **1**, 448–455.
26 H. Baaqel, I. Díaz, V. Tulus, B. Chachuat, G. Guillén-Gosálbez and J. P. Hallett, *Green Chem.*, 2020, **22**, 3132–3140.
27 Y. Zhang, B. R. Bakshi and E. S. Demessie, *Environ. Sci. Technol.*, 2008, **42**, 1724–1730.
28 H. A. Baaqel, A. Bernardi, J. P. Hallett, G. Guillén-Gosálbez and B. Chachuat, *ACS Sustain. Chem. Eng.*, 2023, **11**, 7157–7169.
29 H. Baaqel, J. P. Hallett, G. Guillén-Gosálbez and B. Chachuat, *ACS Sustain. Chem. Eng.*, 2022, **10**, 323–331.
30 P. L. Amado Alviz and A. J. Alvarez, *J. Cleaner Prod.*, 2017, **168**, 1614–1624.
31 Ecoinvent, *Ecoinvent Database V 3.8*, 2025, Available from: https://ecoinvent.org.
32 S. Eini, S. Jhamb, M. Sharifzadeh, D. Rashtchian and G. M. Kontogeorgis, *Chem. Eng. Sci.*, 2020, **226**, 115866.
33 A. S. Hukkerikar, S. Kalakul, B. Sarup, D. M. Young, G. Sin and R. Gani, *J. Chem. Inf. Model.*, 2012, **52**, 2823–2839.
34 A. J. S. McIntosh, J. Griffith and J. Gräsvik, in *Application, Purification, and Recovery of Ionic Liquids*, ed. O. Kuzmina and J. P. Hallett, Elsevier, Amsterdam, 2016, pp. 59–99.
35 A. A. C. Toledo Hijo, G. J. Maximo, M. C. Costa, E. A. C. Batista and A. J. A. Meirelles, *ACS Sustain. Chem. Eng.*, 2016, **4**, 5347–5369.
36 K. Ebel, H. Koehler, A. O. Gamer and R. Jäckh, in *Ullmann's Encyclopedia of Industrial Chemistry*, 2000.
37 T. Shamim, V. Kumar and S. Paul, *Synth. Commun.*, 2014, **44**, 620–632.
38 C. Salis, S. Mohammedi, L. Turazza, Y. Blandin, M. Garnier, C. Hemmert, M. Baltas and H. Gornitzka, *Molecules*, 2025, **30**, 522.
39 T. Erdmenger, J. Vitz, F. Wiesbrock and U. S. Schubert, *J. Mater. Chem.*, 2008, **18**, 5267–5273.
40 J. Feder-Kubis, A. Wnętrzak, J. Suchodolski, P. Tomasz Mitkowski and A. Krasowska, *Chem. Eng. J.*, 2022, **442**, 136062.
41 J. Dupont, C. S. Consorti, P. A. Z. Suarez and R. de Souza, *Org. Synth.*, 2002, **79**, 236.
42 K. R. Seddon, A. Stark and M. J. Torres, *Pure Appl. Chem.*, 2000, **72**, 2275–2287.
43 ISO, *ISO 14040:2006 - Environmental Management — Life Cycle Assessment — Principles and Framework*, 2006.
44 ISO, *ISO 14044:2006 - Environmental Management — Life Cycle Assessment — Requirements and Guidelines*, 2006.
45 E. Igos, A. Dalle, L. Tiruta-Barna, E. Benetto, I. Baudin and Y. Mery, *J. Cleaner Prod.*, 2014, **65**, 424–431.
46 V. G. Maciel, D. J. Wales, M. Seferin, C. M. L. Ugaya and V. Sans, *J. Cleaner Prod.*, 2019, **217**, 844–858.
47 Sphera, LCA For Experts, 2025, Available from: https://sphera.com.
48 H. de Bruijn, R. van Duin, M. A. J. Huijbregts, J. B. Guinee, M. Gorree, R. Heijungs, G. Huppes, R. Kleijn, A. de Koning, L. van Oers, A. Wegener Sleeswijk, S. Suh and H. A. Udo de Haes, in *Handbook on Life Cycle Assessment: Operational Guide to the ISO Standards*, ed. H. de Bruijn, R. van Duin, M. A. J. Huijbregts, J. B. Guinee, M. Gorree, R. Heijungs, G. Huppes, R. Kleijn, A. de Koning, L. van Oers, A. Wegener Sleeswijk, S. Suh and H. A. Udo de Haes, Springer Netherlands, Dordrecht, 2002, pp. 63–95.
49 M. B. Shiflett, *Commercial Applications of Ionic Liquids*, Springer Cham, 2020.
50 S. W. Benson, F. R. Cruickshank, D. M. Golden, G. R. Haugen, H. E. O'Neal, A. S. Rodgers, R. Shaw and R. Walsh, *Chem. Rev.*, 1969, **69**, 279–324.
51 L. Constantinou and R. Gani, *AIChE J.*, 1994, **40**, 1697–1710.
52 R. L. Gardas and J. A. P. Coutinho, *Ind. Eng. Chem. Res.*, 2008, **47**, 5751–5757.
53 R. L. Gardas and J. A. P. Coutinho, *AIChE J.*, 2009, **55**, 1274–1290.

54 A. Vabalas, E. Gowen, E. Poliakoff and A. J. Casson, *PLoS One*, 2019, **14**, e0224365.
55 S. Shalev-Shwartz and S. Ben-David, *Understanding Machine Learning: from Theory to Algorithms*, Cambridge University Press, New York, United States, 2014.
56 M. Kuhn and K. Johnson, *Applied Predictive Modeling*, Springer New York, 2013.
57 Ecoinvent database v 3.5, https://ecoinvent.org/, accessed July 2024.
58 EPA, Evaluation of the Inhalation Carcinogenicity of Ethylene Oxide, U.S. Environmental Protection Agency, Washington, DC, https://cfpub.epa.gov/ncea/iris_drafts/recordisplay.cfm?deid=329730, accessed July 2024.
59 R. van Zelm, M. A. J. Huijbregts and D. van de Meent, *Int. J. Life Cycle Assess.*, 2009, **14**, 282–284.
60 CML, CML-IA Characterisation Factors, Department of Industrial Ecology, Leiden University, https://www.universiteitleiden.nl/en/research/research-output/science/cml-ia-characterisation-factors, accessed July 2024.
61 A. I. Belyanovskaya, B. Laratte, V. D. Rajput, N. Perry and N. V. Baranovskaya, *J. Cleaner Prod.*, 2020, **270**, 122432.
62 ATSDR, *Toxicological profile for Fluorides, Hydrogen Fluoride, and Fluorine, Agency for Toxic Substances and Disease Registry*, Atlanta, GA, U.S. Department of Health and Human Services, Public Health Service, https://wwwn.cdc.gov/TSP/ToxProfiles/ToxProfiles.aspx?id=212&tid=38, accessed July 2024.
63 K. Grodowska and A. Parczewski, *Acta Pol. Pharm.*, 2010, **67**, 3–12.
64 L. Chen, M. Sharifzadeh, N. Mac Dowell, T. Welton, N. Shah and J. P. Hallett, *Green Chem.*, 2014, **16**, 3098–3106.
65 N. Martínez-Ramón, F. Calvo-Rodríguez, D. Iribarren and J. Dufour, *Cleaner Environ. Syst.*, 2024, **14**, 100221.
66 H. Baaqel, J. P. Hallett, G. Guillén-Gosálbez and B. Chachuat, in *Computer Aided Chemical Engineering*, ed. M. Türkay and R. Gani, Elsevier, 2021, vol. 50, pp. 785–790.
67 H. Baaqel, V. Tulus, B. Chachuat, G. Guillén-Gosálbez and J. Hallett, in *Computer Aided Chemical Engineering*, ed. S. Pierucci, F. Manenti, G. L. Bozzano and D. Manca, Elsevier, 2020, vol. 48, pp. 1825–1830.
68 Z. Chen, Z. Li, X. Ma, P. Long, Y. Zhou, L. Xu and S. Zhang, *Green Chem.*, 2017, **19**, 1303–1307.